

Title: Global patterns of forest autotrophic carbon fluxes

Running head: Global patterns of forest carbon fluxes

Authors:

Rebecca Banbury Morgan^{1,2}

Valentine Herrmann¹

Norbert Kunert^{1,3,4}

Ben Bond-Lamberty⁵

Helene C. Muller-Landau³

Kristina J. Anderson-Teixeira^{1,3*}

Institutional Affiliations:

1. Conservation Ecology Center; Smithsonian Conservation Biology Institute; Front Royal, VA, USA

2. School of Geography, University of Leeds, Leeds, UK

3. Center for Tropical Forest Science-Forest Global Earth Observatory; Smithsonian Tropical Research Institute; Panama, Republic of Panama

4. Institute of Botany, University of Natural Resources and Applied Life Sciences, Vienna, Austria

5. Joint Global Change Research Institute, Pacific Northwest National Laboratory, College Park Maryland 20740 USA

*Corresponding Author:

phone: 1-540-635-6546

fax:1-540-635-6506

email: teixeirak@si.edu

Abstract

Carbon (C) fixation, allocation, and metabolism by trees set the basis for energy and material flows in forest ecosystems and define their interactions with Earth's changing climate. However, while many studies have considered variation in productivity with latitude and climate, we lack a cohesive synthesis on how forest carbon fluxes vary globally with respect to climate and one another. Here, we draw upon 1,319 records from the Global Forest Carbon Database (ForC), representing all major forest types and the nine most significant autotrophic carbon fluxes, to comprehensively review how annual C cycling in mature, undisturbed forests varies with latitude and climate on a global scale. We show that, across all flux variables analyzed, C cycling decreases continuously with absolute latitude – a finding that confirms multiple previous studies and contradicts the idea that net primary productivity of temperate forests rivals that of tropical forests. C flux variables generally displayed similar trends across latitude and multiple climate variables, with no differences in allocation detected at this global scale. Temperature variables in general, and mean annual temperature or temperature seasonality in particular, were the single best predictors of C flux, explaining 19 - 71% of variation in the C fluxes analyzed. The effects of temperature were modified by moisture availability, with C flux reduced under hot and dry conditions and sometimes under very high precipitation. Annual C fluxes increased with growing season length and were also influenced by growing season climate. These findings clarify how forest C flux varies with latitude and climate on a global scale. In an era when forests will play a critical yet uncertain role in shaping Earth's rapidly changing climate, our synthesis provides a foundation for understanding global patterns in forest C cycling.

Keywords: carbon fluxes; carbon dioxide (CO₂); climate; forest; global; productivity; respiration; latitude

Introduction

Carbon (C) cycling in Earth’s forests provides the energetic basis for sustaining the majority of Earth’s terrestrial biodiversity and many human populations (Millennium Ecosystem Assessment, 2005), while strongly influencing atmospheric carbon dioxide (CO_2) and climate (Bonan, 2008). Forests’ autotrophic C fluxes – that is, C fixation, allocation, and metabolism by trees and other primary producers – sets the energy ultimately available to heterotrophic organisms (including microbes), in turn influencing their abundance (Niedzialkowska et al., 2010; Zak et al., 1994) and possibly diversity (Chu et al., 2018; Waide et al., 1999). They are linked to cycling of energy, water, and nutrients and, critically, influence all C stocks and define forest interactions with Earth’s changing climate. Each year, over 69 Gt of C cycle through Earth’s forests (Badgley et al., 2019) – a flux more than seven times greater than that of recent anthropogenic fossil fuel emissions (9.5 Gt C yr^{-1} ; Friedlingstein et al., 2019). As atmospheric CO_2 continues to rise, driving climate change, forests will play a critical role in shaping the future of Earth’s climate (Cavaleri et al., 2015; Rogelj et al., 2018). However, our understanding of global-scale variation in forest C cycling remains incomplete, in large part because it is pieced together from numerous studies, most considering only one or a few variables at a time, with various approaches for handling influential factors such as stand age, disturbance history, and management status (Gillman et al., 2015; Litton et al., 2007; Šímová & Storch, 2017).

Forest C fluxes decrease with latitude (e.g., Cramer et al., 1999; Anderson-Teixeira et al., n.d.; Gillman et al., 2015; Li & Xiao, 2019; Luyssaert et al., 2007; Zhao et al., 2005). However, studies have differed in their conclusions regarding the shape of this relationship – quite possibly because of lack of standardization with respect to methodology and stand history. C flux and allocation vary with stand age, disturbance, and management (DeLucia et al., 2007; Fernandez-Martinez et al., 2014; Šímová & Storch, 2017; Yu et al., 2014), making clear latitudinal patterns difficult to discern without standardization of the dataset. Studies agree that gross primary productivity (GPP) increases continuously with decreasing latitude and is indisputably highest in tropical forests (Badgley et al., 2019; Beer et al., 2010; Jung et al., 2011; Li & Xiao, 2019; Luyssaert et al., 2007). However, this relationship is more ambiguous for subsidiary fluxes. Some studies have suggested that net primary productivity (NPP), or its aboveground portion ($ANPP$), exhibits a less distinct increase from temperate to tropical forests (Luyssaert et al., 2007) – or even a decrease (Huston & Wolverton, 2009, but see Gillman et al., 2015). A shallower increase in NPP than in GPP with decreasing latitude would align with the suggestion that tropical forests tend to have low carbon use efficiency ($CUE = NPP/GPP$; DeLucia et al., 2007; Anderson-Teixeira et al., 2016; Malhi, 2012) but contrast with recent findings of the opposite pattern (Collalti et al., 2020). Such differences among C fluxes in their relationship to latitude have profound implications for our understanding of the C cycle and its climate sensitivity (e.g., Collalti

et al., 2020). However, until recently the potential to compare latitudinal trends across C fluxes has been limited by lack of a large database with standardization for methodology, stand history, and management (Anderson-Teixeira et al., n.d., 2018).

Latitudinal gradients in forest C flux rates, along with altitudinal gradients (Girardin et al., 2010; Malhi et al., 2017; Muller-Landau et al., 2020), are driven primarily by climate, which is a significant driver of C fluxes across broad spatial scales (Cleveland et al., 2011; Cramer et al., 1999; Luyssaert et al., 2007; Muller-Landau et al., 2020; Wei et al., 2010). However, there is little consensus as to the shapes of these relationships or the best predictor variables. The majority of studies have focused on exploring the relationships of C fluxes to mean annual temperature (*MAT*) and precipitation (*MAP*), which are the most commonly reported site-level climate variables. C fluxes increase strongly with *MAT* on the global scale, but whether they saturate or potentially decrease at higher temperatures remains disputed. Some studies have detected no deceleration or decline in *GPP* (Luyssaert et al., 2007), *NPP* (Schoor, 2003), or root respiration (R_{root} ; Piao et al., 2010; Wei et al., 2010) with increasing *MAT*. In contrast, others have found evidence of saturation or decline of C flux in the warmest climates: Luyssaert et al. (2007) found *NPP* saturating at around 10°C *MAT*, Larjavaara & Muller-Landau (2012) found that increases in *GPP* saturate at approximately 25°C *MAT*, and Sullivan et al. (2020) found that, within the tropics, woody stem productivity ($ANPP_{stem}$) decreases at the highest maximum temperatures. C fluxes generally saturate at high levels of *MAP*, though the saturation points identified vary widely (e.g., ~1000 - 2,445 mm yr⁻¹; Wei et al., 2010; Schoor, 2003). Interactions between *MAT* and *MAP* may also influence productivity (Beer et al., 2010; Yu et al., 2014); within the tropics, there is a positive interaction between *MAT* and *MAP* in shaping *ANPP*, such that temperature has a positive effect on productivity in moist climates, but a negative effect in dry climates (Taylor et al., 2017). There is also evidence that C fluxes also respond to climate variables such as seasonality of temperature and precipitation (Wagner et al., 2016), cloud cover (Taylor et al., 2017), solar radiation (Beer et al., 2010; Fyllas et al., 2017), and potential evapotranspiration (Kerkhoff et al., 2005); however, these are not typically assessed in global-scale analyses of annual forest C flux.

Mean annual temperature and precipitation do not capture intra-annual climate variation, including temperature and precipitation seasonality and growing season length. Most forests—even tropical evergreen—exhibit some seasonality in both climate and C flux (e.g., Wagner et al., 2014), and this seasonality influences annual C fluxes (Churkina et al., 2005; Fu et al., 2019; Keenan et al., 2014). In particular, growing season length has been linked to *ANPP*, *NPP*, *GPP*, and net ecosystem exchange of CO₂ (*NEE*, or the difference between *GPP* and ecosystem respiration; Kerkhoff et al., 2005; Churkina et al., 2005; Keenan et al., 2014; Michaletz et al., 2014; Zhou et al., 2016). However, the relative importance of growing season length, as opposed to

climate within the growing season, remains debated. On one end of the spectrum, some studies have suggested that the influence of temperature on C fluxes may be limited to determining the length of the frost-free growing season, and that climate within the growing season has little influence on C fluxes because of plant adaptation and acclimatization to local climates (Enquist et al., 2007; Kerkhoff et al., 2005; Michaletz et al., 2018, 2014). In support of this, Kerkhoff et al. (2005) and Michaletz et al. (2014) found no significant relationship between growing season temperature and *ANPP* or *NPP* standardized to a climate-defined growing season length (but see Chu et al., 2016). The idea that growing season length is an important determinant of annual C flux also aligns with evidence that cross-site variation in *NEE* is strongly correlated with growing season length (Churkina et al., 2005) and that warming-induced increases in growing season length are enhancing forest *GPP* and C sequestration (Keenan et al., 2014; Zhou et al., 2016). On the other end of the spectrum, climatic conditions within the growing season may exert a stronger influence on annual C fluxes than the length of the growing season. This aligns with observations that in forests, *NEE* tends to be more closely tied to the maximum rate of CO₂ uptake than to the carbon uptake period (Fu et al., 2019; Zhou et al., 2016), and with numerous tree-ring analyses finding that annual growth is more closely controlled by peak growing season climate than by spring or fall conditions (e.g., Martin-Benito & Pederson, 2015; Helcoski et al., 2019). Thus, the extent to which growing season length controls global-scale variation in forest autotrophic C fluxes remains unclear.

The recent development of the Global Forest Carbon database (ForC), which synthesizes multiple variables and includes records of stand history (Anderson-Teixeira et al., 2016, 2018), opens up the possibility for a standardized analysis of global scale variation in multiple C fluxes and the principle climatic drivers of these patterns. In order to approach this broad topic, we organize the major gaps in our knowledge under five broad review questions and corresponding predictions, many derived from the findings of previous studies (Table 1). First, we ask how nine forest autotrophic carbon fluxes in ForC vary with latitude (*Q1*). We then test how these fluxes relate to *MAT* and *MAP* (*Q2*), and additionally how they respond to other, less well-studied, climate variables (*Q3*). Finally, we consider the relationship between C flux and seasonality, considering the role of seasonality in explaining variation in carbon fluxes (*Q4*), and the influence of climate on C flux standardized by growing season length (*Q5*). Our analyses represent a major step forward in relation to previous work (e.g., Luyssaert et al., 2007) in that we examine global climatic trends in more variables (9 vs. ≤ 3), draw from a much larger database (>4 times more records analyzed), and control for the effects of stand age, disturbance, and management.

Table 1: Summary of review questions, corresponding expectations based on previous studies (when applicable), and results. Statistically significant support for/ rejection of hypotheses is indicated by checkmarks/ X's, whereas '-' indicates no significant relationship. Parentheses indicate partial overall support or rejection of hypotheses across all fluxes considered. Flux variables are defined in Table 2.

| Review questions and hypothesized relationships | Overall | Forest autotrophic carbon fluxes | | | | | | | | | | Support |
|---|---------|----------------------------------|------------|-------------|----------------------------|-------------------------------|-------------|---------------------------------|-------------------------|-------------------------|---|--------------------|
| | | <i>GPP</i> | <i>NPP</i> | <i>ANPP</i> | <i>ANPP_{stem}</i> | <i>ANPP_{foliage}</i> | <i>BNPP</i> | <i>BNPP_{fine.root}</i> | <i>R_{auto}</i> | <i>R_{root}</i> | | |
| Q1. How do C fluxes vary with latitude? | | | | | | | | | | | | |
| continuous increase with decreasing latitude ^{1,2,3} | ✓ | ✓ | ✓ | ✓ | ✓ | ✓ | ✓ | ✓ | ✓ | ✓ | ✓ | Fig. 2 |
| significantly decelerating increase with decreasing latitude ^{1,4} | × | × | × | × | × | × | × | × | × | × | × | Fig. 2 |
| Q2. How do C fluxes vary with mean annual temperature (MAT) and precipitation (MAP)? | | | | | | | | | | | | |
| continuous increase with MAT ^{1,5,6,7} | ✓ | ✓ | ✓ | ✓ | ✓ | ✓ | ✓ | ✓ | ✓ | ✓ | ✓ | Figs. 3, 4, S4, S5 |
| increase with MAP up to ≥ 2000 mm ^{1,4,7} | ✓ | ✓ | ✓ | ✓ | ✓ | ✓ | ✓ | ✓ | ✓ | ✓ | ✓ | Figs. 4, S4, S5 |
| increase with MAT \times MAP ^{8,9} | - | - | × | - | ✓ | - | - | - | - | - | - | Fig. 3, Table S3 |
| Q3. How are C fluxes related to other annual climate variables? | | | | | | | | | | | | |
| decelerating increase or unimodal relationship with PET | ✓ | ✓ | ✓ | ✓ | ✓ | ✓ | ✓ | ✓ | ✓ | ✓ | ✓ | Figs. 4, S4, S5 |
| decelerating increase or unimodal relationship with VPD ¹⁰ | ✓ | ✓ | ✓ | ✓ | ✓ | ✓ | ✓ | ✓ | ✓ | ✓ | ✓ | Figs. 4, S4, S5 |
| increase with solar radiation ^{11,12} | (✓) | ✓ | ✓ | ✓ | ✓ | ✓ | ✓ | ✓ | ✓ | ✓ | - | Figs. S4, S5 |
| Q4. How does seasonality influence annual C fluxes? | | | | | | | | | | | | |
| decrease with temperature seasonality | ✓ | ✓ | ✓ | ✓ | ✓ | ✓ | ✓ | ✓ | ✓ | ✓ | ✓ | Figs. 4, S6, S7 |
| decrease with precipitation seasonality ^{13,14} | - | - | - | - | × | - | - | - | - | - | - | Figs. S6, S7 |
| increase with growing season length ^{15,16,17,18} | ✓ | ✓ | ✓ | ✓ | ✓ | ✓ | ✓ | ✓ | ✓ | ✓ | ✓ | Figs. 4, S6, S7 |
| stronger relationship to growing season length than MAT ^{16,17} | (× | × | × | × | - | × | × | × | × | × | × | Table S4 |
| Q5. When standardised by growing season length, how do annual C fluxes vary with climate? | | | | | | | | | | | | |
| increase with growing season temperature ¹⁷ | (✓) | - | - | ✓ | - | ✓ | - | - | - | - | - | Figs. S8, S9 |
| increase with growing season PET | (✓) | ✓ | ✓ | - | ✓ | - | ✓ | ✓ | - | - | - | Figs. S8, S9 |
| increase with growing season precipitation ¹⁸ | (✓) | - | - | ✓ | - | ✓ | - | - | - | - | - | Figs. S8, S9 |
| increase with growing season solar radiation | (✓) | - | - | - | - | - | ✓ | ✓ | - | - | - | Figs. S8, S9 |

¹ Luyssaert et al. (2007) ² Gillman et al. (2015) ³ Simova and Storch (2017) ⁴ Huston & Wolverton (2009) ⁵ Schuur (2003) ⁶ Piao et al. (2010) ⁷ Wei et al. (2010)
⁸ Taylor et al. (2017) ⁹ Muller-Landau et al. (2020) ¹⁰ Smith et al. (2020) ¹¹ Fyllas et al. (2017) ¹² Nemani et al. (2003) ¹³ Wagner et al. (2014) ¹⁴ Wagner et al. (2016)
¹⁵ Malhi (2012) ¹⁶ Michaletz et al. (2014) ¹⁷ Chu et al. (2016) ¹⁸ Fernandez-Martinez et al. (2014)

Materials and Methods

Forest carbon flux data

This analysis focused on nine C flux variables included in the open-access ForC database (Table 2; Anderson-Teixeira et al., 2016, 2018). ForC contains records of field-based measurements of forest carbon stocks and annual fluxes, compiled from original publications and existing data compilations and databases. Associated data, such as stand age, measurement methodologies, and disturbance history, are also included. The database was significantly expanded since the publication of Anderson-Teixeira et al. (2018) through addition of the Global Soil Respiration Database (Bond-Lamberty & Thomson, 2010; Jian et al., 2020) and the FLUXNET2015 dataset (Pastorello et al., 2020). Additional targeted literature searches were conducted to identify further available data on the fluxes analyzed here, with particular focus on mature forests in temperate and boreal regions, which were not included in the review of Anderson-Teixeira et al. (2016). We used ForC v3.0, archived on Zenodo with DOI 10.5281/zenodo.3403855. This version contained 29,730 records from 4,979 plots, representing 20 distinct ecozones across all forested biogeographic and climate zones. From this, we drew 1,319 records that met our criteria, as outlined below (Fig. 1).

This analysis focused on mature forests with no known history of significant disturbance or management. There is evidence that stand age influences patterns of C flux and allocation in forest ecosystems, and can confound relationships between latitude and primary productivity (DeLucia et al., 2007; Gillman et al., 2015). To reduce any biasing effects of stand age, we included only stands of known age ≥ 100 years and those described by terms such as “mature”, “intact”, or “old-growth”, noting that ages of mature tropical forests are typically unknown because most tropical trees cannot be easily dated using tree-rings. Since management can alter C cycling (Šímová & Storch, 2017), sites were excluded from analysis if they were managed, defined as plots that were planted, managed as plantations, irrigated, fertilised or included the term “managed” in their site description. Sites that had experienced significant disturbance within the past 100 years were also excluded. Disturbances that qualified sites for exclusion included major cutting or harvesting, burning, flooding, drought and storm events with site mortality $>10\%$ of trees. Grazed sites were retained.

Table 2: Definitions and sample sizes of carbon flux variables used in analysis. All variables are in units of $\text{Mg C ha}^{-1} \text{ yr}^{-1}$.

| Variable | Definition | Components included | Methodologies | Sample size | |
|---------------------------------|--------------------------------------|---|--|-------------|-------------------|
| | | | | records | geographic areas* |
| <i>GPP</i> | Gross Primary Production | full ecosystem | flux partitioning of eddy-covariance; $NPP + R_{\text{auto}}$ | 243 | 49 |
| <i>NPP</i> | Net Primary Production | stem, foliage, coarse root, fine root, optionally others (e.g., branch, reproductive, understory) | $ANPP + BNPP$ (majority); $GPP - R_{\text{auto}}$ | 161 | 56 |
| <i>ANPP</i> | Aboveground <i>NPP</i> | stem, foliage, optionally others (e.g., branch, reproductive, understory) | $ANPP_{\text{stem}} + ANPP_{\text{foliage}}$ (+ others) | 278 | 86 |
| <i>ANPP_{stem}</i> | Stem growth component of <i>ANPP</i> | woody stems down to $\text{DBH} \leq 10\text{cm}$ (no branch turnover) | stem growth measurements scaled to biomass using allometries | 264 | 96 |
| <i>ANPP_{foliage}</i> | Foliage component of <i>ANPP</i> | foliage | litterfall collection, with separation into components | 98 | 49 |
| <i>BNPP</i> | Belowground <i>NPP</i> | coarse and fine roots | coarse roots estimated indirectly using allometries based on aboveground stem increment measures ; fine roots as below | 101 | 48 |
| <i>BNPP_{fine.root}</i> | Fine root component of <i>BNPP</i> | fine roots | measurements combined one or more of the following: soil cores, minirhizotrons, turnover estimates, root ingrowth cores | 88 | 41 |
| <i>R_{auto}</i> | Autotrophic respiration | foliage, stem, and root | chamber measurements of foliage and stem gas exchange + R_{root} (as below) | 22 | 13 |
| <i>R_{root}</i> | Root respiration | (coarse and) fine roots | partitioning of total soil respiration (e.g., through root exclusion), scaling of root gas exchange; excluded alkali absorption and soda lime methods for measuring soil respiration | 64 | 26 |

* Geographic areas group geographically proximate sites, defined using a hierarchical cluster analysis on the distance matrix of the sites, and a cutoff of 25km

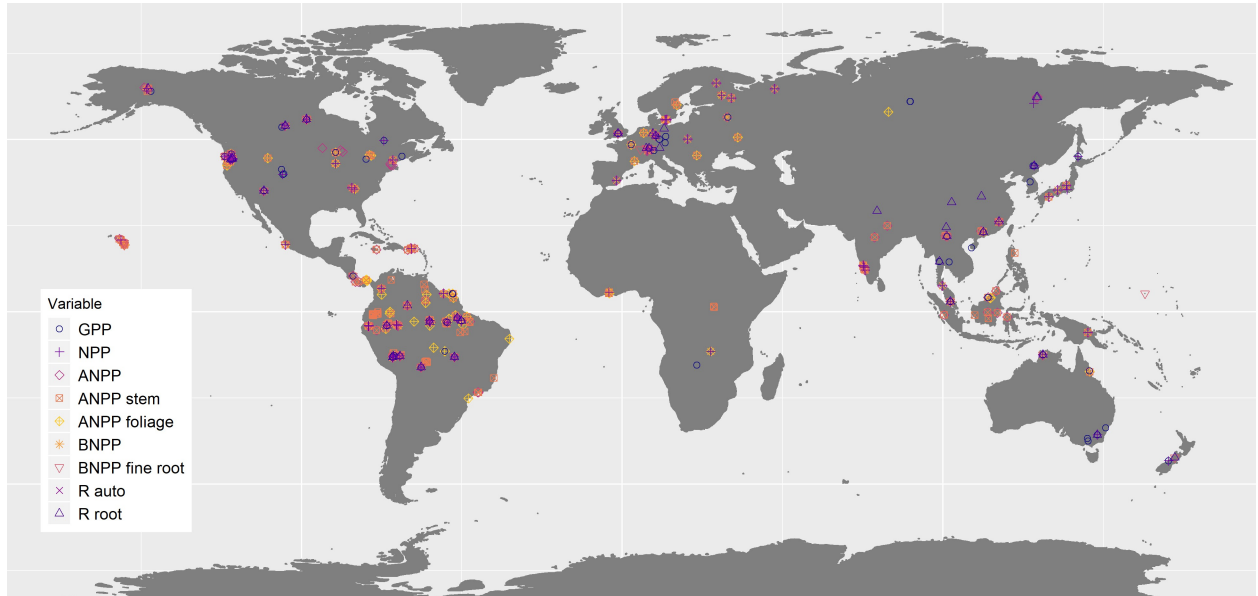


Figure 1: Map showing all data used in the analysis, coded by variable. Variables are plotted individually in Fig. S1.

Climate data

ForC contains geographic coordinates associated with each measurement record and, when available, *MAT* and *MAP* as reported in the primary literature (Anderson-Teixeira et al., 2018). Based on the geographic co-ordinates for each site, data on twelve climate variables – including *MAT*, *MAP*, temperature seasonality (*i.e.*, standard deviation across months), precipitation seasonality (*i.e.*, coefficient of variation of mean monthly precipitation), annual temperature range, solar radiation, cloud cover, annual frost and wet days, potential evapotranspiration (*PET*), aridity (*MAP/PET*), and vapor pressure deficit (*VPD*) – were extracted from five open-access climate datasets: WorldClim (Hijmans et al., 2005), WorldClim2 (Fick & Hijmans, 2017), the Climate Research Unit time-series dataset (CRU TS v4.03 (Harris et al., 2014), the Global Aridity Index and Potential Evapotranspiration Climate Database (Trabucco & Zomer, 2019), and TerraClimate (Abatzoglou et al., 2018) (Table S1). Definitions and methods used to calculate each variable are included in Table S1. From these data, we derived maximum *VPD*, defined as the *VPD* of the month with the largest deficit, and the number of water stress months, defined as the number of months annually where precipitation was lower than *PET*. Where site-level data was missing for *MAT* or *MAP*, we used values from the WorldClim dataset.

Length of the growing season was estimated to the nearest month, where growing season months were defined as months with mean minimum temperature $> 0.5^{\circ}\text{C}$. This is consistent with the previous studies whose hypothesis we were evaluating (Kerkhoff et al., 2005; Michaletz et al., 2014). We experimented with a definition of growing season months including a moisture index, defined as $(MAT - PET)/PET > -0.95$ (Kerkhoff et al., 2005; see also Michaletz et al., 2014). However, we found that including a moisture index had minimal effect on the estimates of growing season length for the sites included here and that the approach performed poorly at defining growing seasons for sites with significant reliance on snow-melt or groundwater, and so chose to exclude this criterion. Monthly data for *PET*, precipitation, and temperature from CRU v 4.03 (Harris et al., 2014) and solar radiation from WorldClim2 (Fick & Hijmans, 2017) were used to calculate mean monthly *PET*, precipitation, temperature and solar radiation during the growing season.

Analyses

The effects of latitude and climate on C fluxes were analysed using mixed effects models using the package ‘lme4’ (Bates et al., 2015) in R v.3.5.1 (R Core Team, 2020). The basic model for all analyses included a fixed effect of latitude or climate and a random effect of plot nested within geographic area. Geographic areas—*i.e.*, spatially clustered sites—were defined within ForC using a hierarchical cluster analysis on the distance matrix of the sites and a cutoff of 25km (Anderson-Teixeira et al., 2018). We experimented with inclusion of altitude as a fixed effect, as productivity is known to decline with elevation in mesic regions (Muller-Landau et al.,

2020), but excluded it from the final models because it added very little explanatory power – that is, the difference in AIC (ΔAIC) relative to models excluding altitude was generally small (often $\Delta AIC < 2$). Effects were considered significant when inclusion of the fixed effect of interest resulted in $p \leq 0.05$ under an ANOVA test, and $\Delta AIC \geq 2.0$ relative to a corresponding null model. All R^2 values presented here are marginal R^2 values, and refer to the proportion of variation explained by only the fixed effects. Specific analyses are as described below.

We first examined the relationship between latitude and C fluxes ($Q1$; Table 1). We tested models with latitude as a first-order linear, second-order polynomial, and logarithmic term. For brevity, we henceforth refer to first-order linear models as “linear” and second-order polynomial models as “polynomial”. We selected as the best model that with the highest ΔAIC relative to a null model with no fixed term, with the qualification that a polynomial model was considered an improvement over a linear model only if it reduced the AIC value by 2.0 or more. In addition, pairwise comparisons of R^2 values were carried out for a selection of pairs of C fluxes to test for differences among variables in the proportion of variation explained by latitude and climate. Models were run on data from sets of sites that were common to each pair, in order to account for variation in the number of data points included. To standardise for variation in degrees of freedom across model types, only linear and logarithmic models were included in the pairwise analysis.

To test whether trends in component fluxes across latitude sum to match those of larger fluxes, regression lines for smaller component fluxes were summed to generate new estimates of larger fluxes. Because no fluxes were significantly better predicted by a logarithmic or polynomial fit than by a linear fit, we used linear fits for all fluxes in this analysis. We then determined whether these summed predictions fell within the 95% CI for the larger flux across the entire latitudinal range. Confidence intervals for the line of best fit for the larger flux were estimated using the ‘bootMer’ function, a parametric bootstrapping method for mixed models (Bates et al., 2015). This function carried out 2000 simulations estimating the line of best fit, using quantiles at 0.025 and 0.975 to estimate 95% CIs. This analysis was applied to the following sets of fluxes: (1) $GPP = NPP + R_{auto}$, (2) $NPP = ANPP + BNPP$, and (3) $ANPP = ANPP_{foliage} + ANPP_{stem}$. In addition, we estimated total belowground C flux (TBCF, not analyzed due to limited data) as $TBCF = BNPP + R_{root}$.

We next examined the relationships of C fluxes to climate variables ($Q2-Q4$; Table 1). We tested first-order linear, second-order polynomial, and logarithmic fits for each climate variable. Again, polynomial fits were considered superior to first-order linear fits only if inclusion of a second-order polynomial term resulted in $\Delta AIC \geq 2.0$ relative to a first-order linear model. We tested relationships of each C flux (Table 2) against each climate variable (Table S1). Variables which were not significant explanatory variables or which explained $< 20\%$ of variation in C fluxes are only presented in SI.

Linear models were used to investigate the potential joint and interactive effects of *MAT* and *MAP* on carbon fluxes (*Q2*; Table 1). An additive model including *MAP* in addition to *MAT* was accepted when $\Delta AIC > 2$ relative to a null including only *MAT* as a fixed effect. An interactive model containing a *MAT* x *MAP* interaction was accepted when $\Delta AIC > 2$ relative to a null including *MAT* and *MAP* as fixed effects.

Variation in allocation to component carbon fluxes was explored for three groupings: (1) $GPP = NPP + R_{auto}$, (2) $NPP = ANPP + BNPP$, and (3) $ANPP = ANPP_{foliage} + ANPP_{stem}$. For each group, measurements taken at the same site and plot, and in the same year, were grouped together. For groups (1) and (2), where 2 of the 3 flux measurements were available for a given site, plot, and year, these measurements were used to calculate the third. We then calculated the ratio of each pair of component fluxes ($NPP : R_{auto}$; $ANPP : BNPP$; $ANPP_{foliage} : ANPP_{stem}$). The logs of these ratios were regressed against latitude, *MAT*, *MAP*, and temperature seasonality, using the linear models specified above. Cook's distance analyses were carried out for each of the models, and extreme outliers removed.

To test whether and how C fluxes varied with climate when standardised by growing season length (*Q5*; Table 1), we first standardized all annual C fluxes by dividing by growing season length (as defined above). We then derived four variables to describe growing season climate (defined to the nearest month): growing season temperature, precipitation, solar radiation, and PET (Table S1). We tested for correlations between these standardised fluxes and growing season climate variables, using only first-order linear models.

All analyses were conducted in R v.3.5.1 (R Core Team, 2020). Code and data necessary to reproduce all results are available through GitHub (https://github.com/forc-db/Global_Productivity) and archived in Zenodo (DOI: TBD).

Results

In total, we analyzed 1,319 records from nine forest autotrophic C flux variables taken from forests that had experienced no major anthropogenic disturbances within the past 100 years. These records represented a total of 255 plots in 154 distinct geographic areas across all forested biogeographic and climate zones (Figs. 1, S1; Table 2).

Q1. How do C fluxes vary with latitude?

All major carbon fluxes decreased with latitude (Fig. 2; Table S2). Latitude was a strong predictor for many of the carbon fluxes, particularly the larger fluxes (Table S2, S6). Latitude explained 64% of variation in GPP ($n = 243$, $p < 0.0001$), 50% in NPP ($n = 161$, $p < 0.0001$) and 44% in ANPP ($n = 278$, $p < 0.0001$). The C fluxes that were most poorly predicted by latitude were $BNPP_{fine.root}$ ($n = 88$, $p < .01$, $R^2 = 0.17$), and

254 $ANPP_{stem}$ ($n = 264$, $p < 0.0001$, $R^2 = 0.18$). The relationship with latitude was best fit by the first-order
 255 linear model, with the exception of NPP and R_{root} , for which a logarithmic model was a slightly – but not
 256 significantly – better fit.

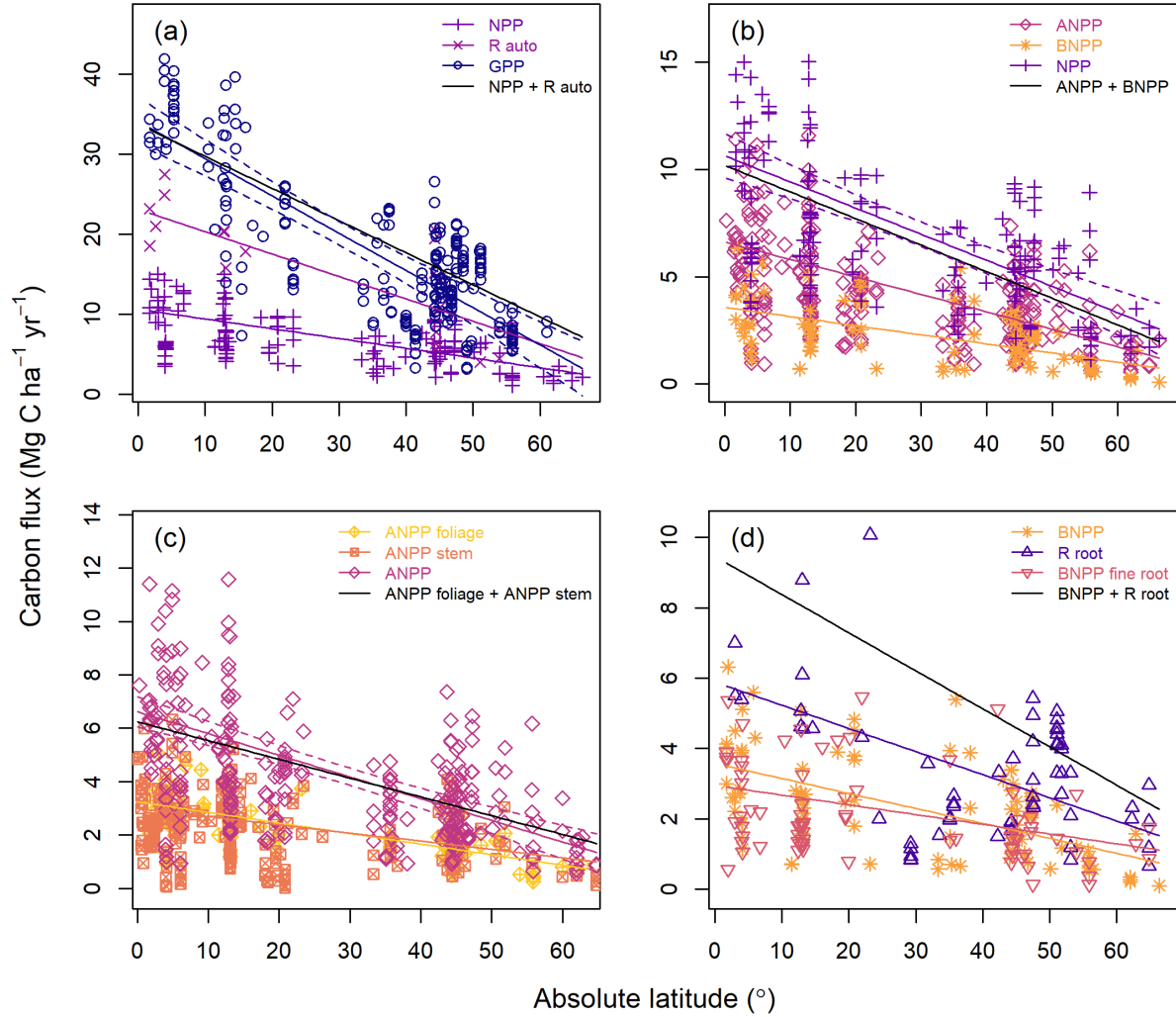


Figure 2: Latitudinal trends in forest autotrophic carbon flux. Plotted are linear models, all of which were significant ($p \leq 0.05$) and had AIC values within 2.0 of the best model (for two fluxes, logarithmic fits were marginally better; Table S2). Sample sizes are available in Table 2 and R^2 values for linear models are available in Table S2. Each panel shows major C fluxes together with component fluxes. Also plotted are predicted trends in the major C fluxes based on the sum of component fluxes. 95% confidence intervals are plotted for the major flux for comparison with predicted trends. In (d), which shows three belowground fluxes, the major flux, total belowground carbon flux, has insufficient data ($n=9$) to support a regression.

257 Smaller component fluxes summed approximately to larger fluxes across the latitudinal gradient (Fig. 2).
 258 That is, modeled estimates of GPP , generated from the sum of NPP and R_{auto} ; NPP , generated from
 259 the sum of $ANPP$ and $BNPP$; and $ANPP$, generated from the sum of $ANPP_{foliage}$ and $ANPP_{stem}$, fell
 260 almost completely within the confidence intervals of the regressions of field estimates of GPP , NPP , and

261 *ANPP*, respectively. An exception was that the summed prediction for $NPP + R_{auto}$ slightly exceeded the
262 upper 95% CI for *GPP* at higher latitudes.

263 We found no evidence of systematic variation in C allocation with latitude or climate (Fig. S3). Of
264 twelve relationships tested (three ratios among C flux variables regressed against latitude, *MAT*, *MAP* and
265 temperature seasonality), none were significant (all $p > 0.05$).

266 *Q2. How do C fluxes relate to MAT and MAP?*

267 All fluxes increased with *MAT* (all $p \leq 0.05$; Figs. 3-4, S4-S5, Table S2). For eight of the nine fluxes, this
268 relationship was linear. For *BNPP* the best fit was a lognormal fit, though this was not significantly better
269 than a linear fit ($\Delta AIC < 2$). As with latitude, *MAT* tended to explain more variation in the larger fluxes
270 (*GPP*, *NPP*, *ANPP*, *R_{auto}*) and *ANPP_{foliage}* (all $R^2 > 0.4$) than in subsidiary and belowground fluxes
271 (*ANPP_{stem}*, *R_{root}*, *BNPP_{fine.root}*; all $R^2 < 0.25$; Table S6).

272 *MAP* was a significant ($p \leq 0.05$) predictor of all fluxes (Figs. 4a, S4-S5; Table S2). However, with the
273 exception of *R_{auto}*, *MAP* explained at most 25% of variation in C flux. All fluxes increased with *MAP* up
274 to at least 2000 mm, above which responses were variable (Figs. 4, S4-S5).

275 There was a significant additive effect of *MAT* and *MAP* on *GPP*, *ANPP* and *R_{auto}* (Fig. 3, Table S3), and
276 a significant interactive effect between *MAT* and *MAP* for *NPP* and *ANPP_{stem}* (Fig. 3, Table S3). The
277 interaction was negative for *NPP* and positive for *ANPP_{stem}*. For *ANPP_{foliage}*, *BNPP*, *BNPP_{fine.root}*,
278 and *R_{root}*, *MAP* did not have a significant effect when accounting for *MAT* (Fig. 3, Table S3).

286 a logarithmic relationship with VPD , but all other fluxes showed a polynomial relationship (Figs. 4d, S4-5;
287 Table S2). C fluxes initially increased with VPD , before saturating at around 0.8 kPa, after which point
288 they began to decrease.

289 All fluxes, with the exception of R_{root} , showed a significant positive relationship with solar radiation (Figs.
290 S4-S5, Table S2). Solar radiation explained a low proportion of variability (<30%) in all C fluxes.

291 Annual wet days, cloud cover, and aridity were poor or non-significant predictors of variation in C fluxes,
292 explaining less than 20% of the variation in each of the carbon fluxes (Figs. S4-S5; Table S2).

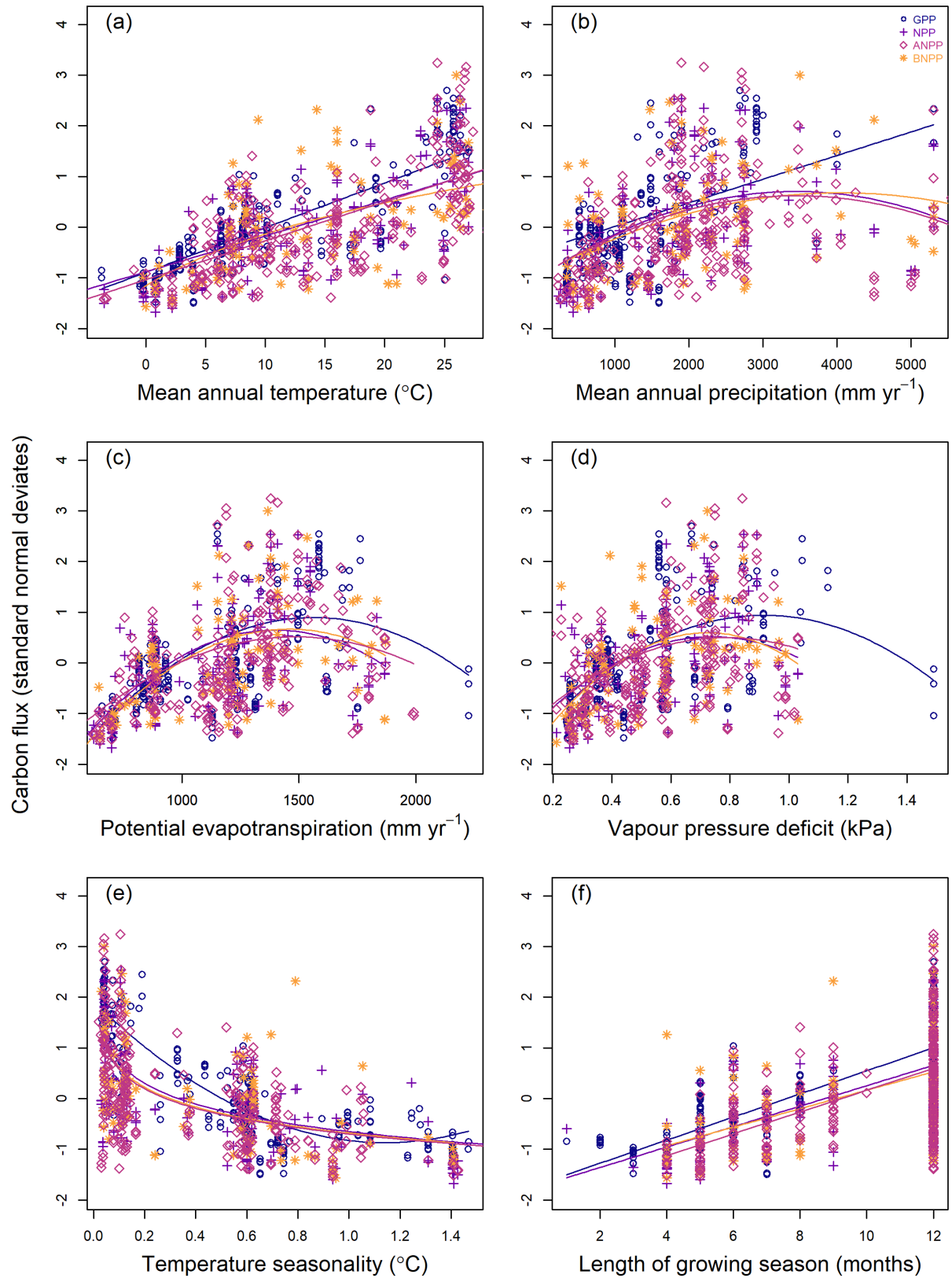


Figure 4: Plots of carbon fluxes against (a) mean annual temperature; (b) mean annual precipitation; (c) potential evapotranspiration, (d) vapour pressure deficit; (e) temperature seasonality; (f) length of growing season. For visualization purposes, data for each flux was rescaled with a mean of 0 and standard deviation of 1. Lines of best fit are plotted according to the best model selected during analysis. All regressions are significant ($p \leq 0.05$). Sample sizes are available in Table 2 and R^2 values are available in Table S2.

Q4. What is the role of seasonality in explaining C fluxes?

Variables describing temperature seasonality – temperature seasonality, annual temperature range, annual frost days, and length of growing season – were strongly correlated with both latitude and *MAT* (all $r \geq 0.2$; Fig. S2), and were consistently identified as strong univariate predictors of C fluxes (Figs. 4, S4-S7).

All fluxes decrease with increasing temperature seasonality, though the shape of this relationship varies (all $p \leq 0.05$; Figs. 4e, S6-7; Table S2). Temperature seasonality was strongly correlated with annual temperature range, which was likewise a similarly strong predictor of C fluxes (Table S2). C fluxes were highest in regions with low seasonality, indicated by temperature seasonality = 0, and annual temperature range $\leq 15^\circ\text{C}$ (*i.e.*, in the tropics).

In contrast, there was no significant effect of precipitation seasonality on C fluxes at this global scale. Both maximum vapour pressure deficit and water stress months were poor or non-significant predictors of variation in C fluxes (Figs. S6-S7; Table S2).

We found a significant relationship between length of growing season and C fluxes, with all fluxes showing a positive relationship with length of growing season (Figs. 4e, S6-S7; Table S2). Length of growing season was a strong predictor of C fluxes, explaining 53% of variation in GPP, 38% of variation in NPP, and 34% of variation in ANPP (all $p \leq 0.05$; Table S2), but it was a weaker predictor than *MAT* for all fluxes analysed (Table S4).

Q5. Within the growing season, how do C fluxes vary with climate?

When annual C fluxes were standardized by growing season length (in integer number of months), correlations with growing season climate were generally weak (Figs. S8-S9). *ANPP* increased with growing season temperature ($R^2 = 0.09$, $p < 0.001$) and precipitation ($R^2 = 0.04$, $p \leq 0.05$). Similarly, *ANPP_{foliage}* increased slightly with growing season temperature ($R^2 = 0.16$, $p < 0.01$) and precipitation ($R^2 = 0.09$, $p \leq 0.05$). Growing season solar radiation was positively correlated with *BNPP* ($R^2 = 0.17$, $p < 0.001$) and *BNPP_{fine.root}* ($R^2 = 0.13$, $p < 0.01$). Growing season PET had a positive influence on *GPP* ($R^2 = 0.15$, $p < 0.01$), *NPP* ($R^2 = 0.07$, $p < 0.01$), *BNPP* ($R^2 = 0.23$, $p < 0.0001$), *BNPP_{fine.root}* ($R^2 = 0.10$, $p \leq 0.05$), and *ANPP_{stem}* ($R^2 = 0.06$, $p \leq 0.05$). All other relationships were non-significant ($p > 0.05$).

Discussion

Our analysis of a large global database (ForC) clarifies how autotrophic C fluxes in mature forests vary with latitude and climate on a global scale (Table 1). We show that, across all nine variables analyzed, annual C flux decreases continually with latitude (Fig. 2), a finding that confirms multiple previous studies and

contradicts the idea that productivity of temperate forests rivals or even exceeds that of tropical forests (Huston & Wolverton, 2009; Luyssaert et al., 2007). At this global scale, C fluxes increase approximately in proportion to one another, with component fluxes summing appropriately to larger fluxes and no detectable differences in allocation across latitude or climates (Figs. 2, 4, S3). Similarly, we show broad - *albeit* not complete - consistency of climate responses across C fluxes, with the observed latitudinal variation primarily attributable to temperature and its seasonality (Figs. 3-4). Water availability is also influential, but of secondary importance across the climate space occupied by forests (Figs. 3-4). Contrary to prior suggestions that the majority of variation in C cycling is driven primarily by the length of the growing season (Enquist et al., 2007; Kerkhoff et al., 2005; Michaletz et al., 2014), we find modest explanatory power of growing season length and small but sometimes significant influences of growing season climate (Figs. 4f, S6-S9). Together, these findings yield a unified understanding of climate’s influence on forest C cycling.

Our findings indicate that, among mature, undisturbed stands, forest C fluxes are unambiguously highest in the tropical regions, and the relationship with both latitude and *MAT* is approximately linear (Table 1, *Q1, Q2*; Figs. 2, 4). This contrasts with the suggestion that C fluxes (e.g., *NPP*, *ANPP*, *ANPP_{stem}*) of temperate forests are similar to or even greater than that of tropical forests (Huston & Wolverton, 2009; Luyssaert et al., 2007). Previous indications of this pattern may have been an artifact of differences in stand age across biomes. Compared to tropical forests, the temperate forest biome has experienced more widespread anthropogenic disturbance and has a larger fraction of secondary stands (Potapov et al., 2008; Poulter et al., 2018; Yu et al., 2014), so analyses comparing across latitudinal gradients without controlling for stand age risk confounding age with biome effects. Because carbon allocation varies with stand age (Anderson-Teixeira et al., n.d., 2013; DeLucia et al., 2007; Doughty et al., 2018), age differences may introduce systematic biases into analyses of C fluxes across latitude or global climatic gradients. For example, woody productivity tends to be higher in rapidly aggrading secondary stands than in old-growth forests, where proportionally more C is allocated to respiration and non-woody productivity (DeLucia et al., 2007; Doughty et al., 2018; Kunert et al., 2019; Piao et al., 2010). Thus, findings that temperate forest productivity rivals that of tropical forests are likely an artifact of different forest ages across biomes. The significant variation in C fluxes as a function of stand age has implications for ecosystem models. Ecosystem modelling approaches may neglect age-related effects, or assume stand equilibrium (see e.g. Yu et al., 2014; Collalti et al., 2020). Our results highlight the importance of incorporating stand age into ecosystem models; without this, models are likely to be vulnerable to bias in global C flux projections.

We show that C fluxes are broadly consistent in their responses to climate drivers on the global scale, with no significant trends in C allocation among the variable pairs tested (Figs. 2, S3). This parallels the observation

that C allocation across multiple C fluxes varies little with respect to climate along a steep tropical elevational gradient (Malhi et al., 2017; but see Moser et al., 2011), and is not surprising given that carbon allocation within forest ecosystems is relatively constrained (Collalti et al., 2020; Enquist, 2002; Litton et al., 2007; Malhi et al., 2011). We find no significant trend in the allocation of GPP between production and respiration across latitude or climate ($NPP:R_{auto}$; Fig. S3), counter to the idea that tropical forests have anomalously low CUE (Anderson-Teixeira et al., 2016; DeLucia et al., 2007; Malhi, 2012), as predicted by most models (Collalti et al., 2020). In contrast, Collalti et al. (2020) found that forest production efficiency increased with temperature—a finding that is consistent in direction with insignificant trends observed here (Fig. S3).

Previously observed differences in CUE between old-growth tropical forests relative to (mostly younger) extratropical forests are likely an artifact of comparing stands of different age, as CUE declines with forest age (Collalti et al., 2020; DeLucia et al., 2007; Piao et al., 2010). Another previously observed pattern for which we find no support is a tendency for belowground C allocation to decrease with increasing temperature (Gill & Finzi, 2016; Moser et al., 2011; Xia et al., 2019); rather, we observe no trends in allocation between $ANPP$ and $BNPP$ across latitudes. Failure to detect significant trends in C allocation with respect to climate in this analysis does not imply that none exist; rather, it suggests that, at this global scale, differences are subtle and/or that more careful methodological standardization and/or more data is required to detect them (*sensu* Collalti et al., 2020).

Despite the broad consistency of climate responses across C fluxes, climate explains lower proportions of variability among some of the subsidiary C fluxes (*e.g.*, $ANPP_{stem}$, $BNPP$, $BNPP_{fine.root}$; Fig. 2; Tables S2, S6). There are two, non-exclusive, potential explanations for this. First, it may be that methodological variation is larger relative to flux magnitude for some of the subsidiary fluxes. Belowground fluxes in particular are difficult to quantify, and measurement methods for the belowground fluxes considered here may use fundamentally different approaches in different sites (*e.g.*, minirhizotrons, ingrowth cores, or sequential coring for $BNPP_{fine.root}$; root exclusion, stable isotope tracking, or gas exchange of excised roots for R_{root}), and sampling depth is variable and often insufficient to capture the full soil profile. $ANPP_{stem}$, which is also poorly explained by latitude or climate, is more straightforward to estimate but subject to variability introduced by methodological differences including minimum plant size sampled and choice of biomass allometries (Clark et al., 2001). That said, methodological variation and uncertainty affect all of fluxes considered here, and some of the larger fluxes that vary more strongly with respect to climate ($ANPP$, NPP) are estimated by summing uncertain component fluxes. Second, differences among variables in the proportion of variation explained by climate may be attributable to more direct climatic control over GPP than subsidiary fluxes. That is, subsidiary fluxes may be shaped by climate both through its influence on GPP and through its

influence on *CUE* and C allocation, as is imbued in the structure of most models (Cramer et al., 1999; Šímová & Storch, 2017).

Temperature and its seasonality were the primary drivers of C fluxes on the global scale (Table 1, *Q2*, *Q4*; Figs. 2-4), consistent with a long legacy of research identifying temperature as a primary driver of forest ecosystem C cycling (e.g., Lieth, 1973; Luyssaert et al., 2007; Wei et al., 2010). We find little evidence of any non-linearity in temperature’s influence on C fluxes. The relationship of all fluxes to *MAT* as an individual driver were best described by a linear function (Table S2) – with the exception of *BNPP*, whose response to *MAT* was close to linear (Fig. 4a). This result contrasts with previous findings of fluxes saturating with *MAT* below approximately 25°C *MAT* (Huston & Wolverton, 2009; Luyssaert et al., 2007). It remains possible that fluxes decline above this threshold (Larjavaara & Muller-Landau, 2012; Sullivan et al., 2020). However, these higher temperatures also tend to be associated with high *PET* and *VPD*, both of which are associated with reduced C fluxes (Figs. 4c-d, S4-S5; Slot & Winter, 2018).

Indeed, while temperature responses dominate at this global scale and within the climate space occupied by forests, the effects of temperature are moderated by moisture availability (Table 1, *Q2*, *Q3*; Figs 3-4). Specifically, C fluxes are reduced under relatively dry conditions (*i.e.*, low *MAP*; high *VPD*) and sometimes under very high precipitation (Figs. 3-4). The observed positive interaction between *MAT* and *MAP* for *ANPP_{stem}* on the global scale (Fig. 3) is consistent with an analysis showing a similar interaction for *ANPP* in tropical forests, also with a cross-over point at ~20°C (Taylor et al., 2017). However, we detect no such interaction for *ANPP* or most other C fluxes, and we find a contrasting negative interaction for *NPP* (Fig. 3), suggesting that more data are required to sort out potential differences in the interactive effects of *MAT* and *MAP* on C fluxes in the tropics.

Forest C fluxes decline with temperature seasonality (Table 1, *Q4*; Fig. 4e), as is to be expected given that fluxes are minimal during winters. A temperature-defined growing season length correlated with global-scale variation in annual C flux (Table 1, *Q5*; Fig. 4f; see also Churkina et al., 2005), consistent with the idea that the latitudinal gradient in carbon flux is attributable more to shorter growing seasons at high latitudes than to inherently lower rates of photosynthesis or respiration by high-latitude forests (Enquist et al., 2007; Fu et al., 2019). However, we find evidence that, within the growing season, climate still plays an important role in shaping C fluxes, as indicated by a number of positive correlations between monthly mean flux during the growing season and growing season temperature, solar radiation, and *PET* (Table 1, Figs. S8-S9). This suggests that, while trees in high-latitude forests have adaptations to maximize photosynthesis at low temperatures (Helliker & Richter, 2008; Huang, 2019), such adaptations are not sufficient to yield growing season fluxes comparable to those of tropical forests. Thus, we reject the hypothesis that there is

no relationship between C flux per month of the growing season and growing season climatic conditions (Table 1, *Q5*; Kerkhoff et al., 2005; Enquist et al., 2007; Michaletz et al., 2014). Rather, annual C flux is shaped by both growing season length and the climate of peak growing season months (Chu et al., 2016; Fu et al., 2019). Given strong co-variation between growing season length and *MAT* (Fig. S2; Chu et al., 2016), accurately partitioning their influence will require data on intra-annual variation in C flux coupled with a higher-precision metric of growing season length than the monthly-resolution metric used here (e.g., based on leaf phenology or C exchange, *sensu* Fu et al., 2019). Fu et al. (2019) find that global-scale geographic variation in annual *NEE* is driven more strongly by growing season length than by carbon uptake rates within the growing season, whereas interannual variation in *NEE* and *GPP* at any given site appears to be driven predominantly by the maximum rate of C uptake, as opposed to growing season length (Fu et al., 2019; Zani et al., 2020; Zhou et al., 2016). Further analysis of interannual variation in C fluxes in relation to climate will be valuable in disentangling how seasonality shapes broad geographic patterns in forest C flux.

Our analysis clarifies how annual forest autotrophic C fluxes vary with latitude and climate on a global scale. To the extent that patterns across broad scale climatic gradients can foretell ecosystem responses to climate change, our findings suggest that higher temperatures with similar moisture availability would result in a generalized acceleration of forest C cycling (Figs. 2-3). This is consistent with observations of continental- to global-scale increases over time in *GPP* (Li & Xiao, 2019), *ANPP_{stem}* (Brienen et al., 2015; Hubau et al., 2020), tree mortality (Brienen et al., 2015; McDowell et al., 2018), soil respiration (Bond-Lamberty & Thomson, 2010), and heterotrophic soil respiration (Bond-Lamberty et al., 2018). However, increasing C flux rates are by no means universal (e.g., Rutishauser et al., 2020; Hubau et al., 2020), likely because other factors are at play, including changes to other aspects of climate, atmospheric pollution (CO_2 , SO_2 , NO_x), and local disturbances. Moreover, forest ecosystem responses to climatic changes outside the temperature range to which forest communities are adapted and acclimatized will not necessarily parallel responses across geographic gradients in climate (e.g., Klesse et al., 2020). Indeed, tree-ring studies from forests around the world indicate that tree growth rates – along with *ANPP_{stem}* and possibly other ecosystem C fluxes – often respond negatively to growing season temperature, particularly in warmer climates (e.g., Helcoski et al., 2019; Klesse et al., 2018; Martin-Benito & Pederson, 2015; Vlam et al., 2014). Furthermore, in the tropics, climate change will push temperatures beyond any contemporary climate, and there are some indications that this could reduce forest C flux rates (Mau et al., 2018; Sullivan et al., 2020) if paralleled by *VPD* increases (Smith et al., 2020). Further research is required to understand the extent to which forest responses to climate change will track the observed global gradients, and the time scale on which they will do so. In the meantime, understanding the fundamental climatic controls on annual C cycling in Earth’s forests sets a

firmer foundation for understanding global-scale forest C cycling and benchmarking the models (Fer et al., 2021) used to predict forest responses and feedbacks to accelerating climate change.

Acknowledgements

We gratefully acknowledge all authors of the original studies and data compilations included in this analysis, their funding agencies, and the various networks that support ground-based measurements of C fluxes. We also thank the numerous researchers who have contributed to the building of ForC. This manuscript was improved by comments from two anonymous reviewers. This study was funded by a Smithsonian Scholarly Studies grant to KJAT and HCML and by Smithsonian’s Forest Global Earth Observatory (ForestGEO). Original compilation of the ForC database was funded by DOE grants DE-SC0008085 and DE-SC0010039 to KAT.

References

- Abatzoglou, J. T., Dobrowski, S. Z., Parks, S. A., & Hegewisch, K. C. (2018). TerraClimate, a high-resolution global dataset of monthly climate and climatic water balance from 1958–2015. *Scientific Data*, 5(1), 170191. <https://doi.org/10.1038/sdata.2017.191>
- Anderson-Teixeira, K., Herrmann, V., Banbury Morgan, B., Bond-Lamberty, B. P., Cook-Patton, S. C., Ferson, A. E., Muller-Landau, H. C., & Wang, M. M. H. (n.d.). Carbon cycling in mature and regrowth forests globally. *Environmental Research Letters*.
- Anderson-Teixeira, K. J., Miller, A. D., Mohan, J. E., Hudiburg, T. W., Duval, B. D., & DeLucia, E. H. (2013). Altered dynamics of forest recovery under a changing climate. *Global Change Biology*, 19(7), 2001–2021. <https://doi.org/10.1111/gcb.12194>
- Anderson-Teixeira, K. J., Wang, M. M. H., McGarvey, J. C., Herrmann, V., Tepley, A. J., Bond-Lamberty, B., & LeBauer, D. S. (2018). ForC: A global database of forest carbon stocks and fluxes. *Ecology*, 99(6), 1507–1507. <https://doi.org/10.1002/ecy.2229>
- Anderson-Teixeira, K. J., Wang, M. M. H., McGarvey, J. C., & LeBauer, D. S. (2016). Carbon dynamics of mature and regrowth tropical forests derived from a pantropical database (TropForC-db). *Global Change Biology*, 22(5), 1690–1709. <https://doi.org/10.1111/gcb.13226>
- Badgley, G., Anderegg, L. D. L., Berry, J. A., & field, C. B. (2019). Terrestrial gross primary production: Using NIR ν to scale from site to globe. *Global Change Biology*, 25(11), 3731–3740. <https://doi.org/10.1111/gcb.14729>

480 Bates, D., Mächler, M., Bolker, B., & Walker, S. (2015). Fitting Linear Mixed-Effects Models Using **lme4**.
481 *Journal of Statistical Software*, 67(1). <https://doi.org/10.18637/jss.v067.i01>

482 Beer, C., Reichstein, M., Tomelleri, E., Ciais, P., Jung, M., Carvalhais, N., Rodenbeck, C., Arain, M. A.,
483 Baldocchi, D., Bonan, G. B., Bondeau, A., Cescatti, A., Lasslop, G., Lindroth, A., Lomas, M., Luyssaert, S.,
484 Margolis, H., Oleson, K. W., Rouspard, O., . . . Papale, D. (2010). Terrestrial Gross Carbon Dioxide Uptake:
485 Global Distribution and Covariation with Climate. *Science*, 329(5993), 834–838. [https://doi.org/10.1126/](https://doi.org/10.1126/science.1184984)
486 [science.1184984](https://doi.org/10.1126/science.1184984)

487 Bonan, G. B. (2008). Forests and Climate Change: Forcings, Feedbacks, and the Climate Benefits of Forests.
488 *Science*, 320(5882), 1444–1449. <https://doi.org/10.1126/science.1155121>

489 Bond-Lamberty, B., Bailey, V. L., Chen, M., Gough, C. M., & Vargas, R. (2018). Globally rising soil
490 heterotrophic respiration over recent decades. *Nature*, 560(7716), 80–83. [https://doi.org/10.1038/s41586-](https://doi.org/10.1038/s41586-018-0358-x)
491 [018-0358-x](https://doi.org/10.1038/s41586-018-0358-x)

492 Bond-Lamberty, B., & Thomson, A. (2010). A global database of soil respiration data. *Biogeosciences*, 7(6),
493 1915–1926. <https://doi.org/10.5194/bg-7-1915-2010>

494 Brien, R. J. W., Phillips, O. L., Feldpausch, T. R., Gloor, E., Baker, T. R., Lloyd, J., Lopez-Gonzalez, G.,
495 Monteagudo-Mendoza, A., Malhi, Y., Lewis, S. L., Vásquez Martinez, R., Alexiades, M., Álvarez Dávila, E.,
496 Alvarez-Loayza, P., Andrade, A., Aragão, L. E. O. C., Araujo-Murakami, A., Arets, E. J. M. M., Arroyo,
497 L., . . . Zagt, R. J. (2015). Long-term decline of the Amazon carbon sink. *Nature*, 519(7543), 344–348.
498 <https://doi.org/10.1038/nature14283>

499 Cavaleri, M. A., Reed, S. C., Smith, W. K., & Wood, T. E. (2015). Urgent need for warming experiments in
500 tropical forests. *Global Change Biology*, 21(6), 2111–2121. <https://doi.org/10.1111/gcb.12860>

501 Chu, C., Bartlett, M., Wang, Y., He, F., Weiner, J., Chave, J., & Sack, L. (2016). Does climate directly
502 influence NPP globally? *Global Change Biology*, 22(1), 12–24. <https://doi.org/10.1111/gcb.13079>

503 Chu, C., Lutz, J. A., Král, K., Vrška, T., Yin, X., Myers, J. A., Abiem, I., Alonso, A., Bourg, N., Burslem, D.
504 F., Cao, M., Chapman, H., Condit, R., Fang, S., Fischer, G. A., Gao, L., Hao, Z., Hau, B. C., He, Q., . . . He,
505 F. (2018). Direct and indirect effects of climate on richness drive the latitudinal diversity gradient in forest
506 trees. *Ecology Letters*, ele.13175. <https://doi.org/10.1111/ele.13175>

507 Churkina, G., Schimel, D., Braswell, B. H., & Xiao, X. (2005). Spatial analysis of growing season length control
508 over net ecosystem exchange. *Global Change Biology*, 11(10), 1777–1787. [https://doi.org/10.1111/j.1365-](https://doi.org/10.1111/j.1365-2486.2005.001012.x)
509 [2486.2005.001012.x](https://doi.org/10.1111/j.1365-2486.2005.001012.x)

510 Clark, D. A., Brown, S., Kicklighter, D. W., Chambers, J. Q., Thomlinson, J. R., & Ni, J. (2001). Measuring
 511 net primary production in forests: Concepts and field methods. *Ecological Applications*, 11(2), 15.

512 Cleveland, C. C., Townsend, A. R., Taylor, P., Alvarez-Clare, S., Bustamante, M. M. C., Chuyong, G.,
 513 Dobrowski, S. Z., Grierson, P., Harms, K. E., Houlton, B. Z., Marklein, A., Parton, W., Porder, S., Reed, S.
 514 C., Sierra, C. A., Silver, W. L., Tanner, E. V. J., & Wieder, W. R. (2011). Relationships among net primary
 515 productivity, nutrients and climate in tropical rain forest: A pan-tropical analysis: Nutrients, climate and
 516 tropical NPP. *Ecology Letters*, 14(9), 939–947. <https://doi.org/10.1111/j.1461-0248.2011.01658.x>

517 Collalti, A., Ibrom, A., Stockmarr, A., Cescatti, A., Alkama, R., Fernández-Martínez, M., Matteucci, G.,
 518 Sitch, S., Friedlingstein, P., Ciais, P., Goll, D. S., Nabel, J. E. M. S., Pongratz, J., Arneeth, A., Haverd,
 519 V., & Prentice, I. C. (2020). Forest production efficiency increases with growth temperature. *Nature*
 520 *Communications*, 11(1), 5322. <https://doi.org/10.1038/s41467-020-19187-w>

521 Cramer, W., Kicklighter, D. W., Bondeau, A., Iii, B. M., Churkina, G., Nemry, B., Ruimy, A., Schloss, A.
 522 L., & Intercomparison, T. P. O. T. P. N. M. (1999). Comparing global models of terrestrial net primary
 523 productivity (npp): Overview and key results. *Global Change Biology*, 5(S1), 1–15. <https://doi.org/https://doi.org/10.1046/j.1365-2486.1999.00009.x>
 524

525 DeLucia, E. H., Drake, J. E., Thomas, R. B., & Gonzalez-Meler, M. (2007). Forest carbon use efficiency:
 526 Is respiration a constant fraction of gross primary production? *Global Change Biology*, 13(6), 1157–1167.
 527 <https://doi.org/10.1111/j.1365-2486.2007.01365.x>

528 Doughty, C. E., Goldsmith, G. R., Raab, N., Girardin, C. A. J., Farfan-Amezquita, filio, Huaraca-Huasco, W.,
 529 Silva-Espejo, J. E., Araujo-Murakami, A., Costa, A. C. L. da, Rocha, W., Galbraith, D., Meir, P., Metcalfe,
 530 D. B., & Malhi, Y. (2018). What controls variation in carbon use efficiency among Amazonian tropical
 531 forests? *Biotropica*, 50(1), 16–25. <https://doi.org/10.1111/btp.12504>

532 Enquist, B. J. (2002). Global Allocation Rules for Patterns of Biomass Partitioning in Seed Plants. *Science*,
 533 295(5559), 1517–1520. <https://doi.org/10.1126/science.1066360>

534 Enquist, B. J., Kerkhoff, A. J., Huxman, T. E., & Economo, E. P. (2007). Adaptive differences in plant
 535 physiology and ecosystem paradoxes: Insights from metabolic scaling theory. *Global Change Biology*, 13(3),
 536 591–609. <https://doi.org/10.1111/j.1365-2486.2006.01222.x>

537 Fer, I., Gardella, A. K., Shiklomanov, A. N., Campbell, E. E., Cowdery, E. M., De Kauwe, M. G., Desai,
 538 A., Duveneck, M. J., Fisher, J. B., Haynes, K. D., Hoffman, F. M., Johnston, M. R., Kooper, R., LeBauer,
 539 D. S., Mantooth, J., Parton, W. J., Poulter, B., Quaife, T., Raiho, A., ... Dietze, M. C. (2021). Beyond

ecosystem modeling: A roadmap to community cyberinfrastructure for ecological data-model integration. *Global Change Biology*, 27(1), 13–26. <https://doi.org/https://doi.org/10.1111/gcb.15409>

Fernandez-Martinez, M., Vicca, S., Janssens, I. A., Luyssaert, S., Campioli, M., Sardans, J., & Estiarte, M. (2014). *Spatial variability and controls over biomass stocks, carbon fluxes, and resource-use efficiencies across forest ecosystems*. 15.

Fick, S. E., & Hijmans, R. J. (2017). WorldClim 2: New 1-km spatial resolution climate surfaces for global land areas: New climate surfaces for global land areas. *International Journal of Climatology*, 37(12), 4302–4315. <https://doi.org/10.1002/joc.5086>

Friedlingstein, P., Jones, M. W., O’Sullivan, M., Andrew, R. M., Hauck, J., Peters, G. P., Peters, W., Pongratz, J., Sitch, S., Le Quéré, C., Bakker, D. C. E., Canadell, J. G., Ciais, P., Jackson, R. B., Anthoni, P., Barbero, L., Bastos, A., Bastrikov, V., Becker, M., ... Zaehle, S. (2019). Global Carbon Budget 2019. *Earth System Science Data*, 11(4), 1783–1838. <https://doi.org/10.5194/essd-11-1783-2019>

Fu, Z., Stoy, P. C., Poulter, B., Gerken, T., Zhang, Z., Wakbulcho, G., & Niu, S. (2019). Maximum carbon uptake rate dominates the interannual variability of global net ecosystem exchange. *Global Change Biology*, 25(10), 3381–3394. <https://doi.org/10.1111/gcb.14731>

Fyllas, N. M., Bentley, L. P., Shenkin, A., Asner, G. P., Atkin, O. K., Díaz, S., Enquist, B. J., Farfan-Rios, W., Gloor, E., Guerrieri, R., Huasco, W. H., Ishida, Y., Martin, R. E., Meir, P., Phillips, O., Salinas, N., Silman, M., Weerasinghe, L. K., Zaragoza-Castells, J., & Malhi, Y. (2017). Solar radiation and functional traits explain the decline of forest primary productivity along a tropical elevation gradient. *Ecology Letters*, 20(6), 730–740. <https://doi.org/10.1111/ele.12771>

Gill, A. L., & Finzi, A. C. (2016). Belowground carbon flux links biogeochemical cycles and resource-use efficiency at the global scale. *Ecology Letters*, 19(12), 1419–1428. <https://doi.org/10.1111/ele.12690>

Gillman, L. N., Wright, S. D., Cusens, J., McBride, P. D., Malhi, Y., & Whittaker, R. J. (2015). Latitude, productivity and species richness: Latitude and productivity. *Global Ecology and Biogeography*, 24(1), 107–117. <https://doi.org/10.1111/geb.12245>

Girardin, C. A. J., Malhi, Y., Aragão, L. E. O. C., Mamani, M., Huaraca Huasco, W., Durand, L., Feeley, K. J., Rapp, J., Silva-Espejo, J. E., Silman, M., Salinas, N., & Whittaker, R. J. (2010). Net primary productivity allocation and cycling of carbon along a tropical forest elevational transect in the Peruvian Andes: NET PRIMARY PRODUCTIVITY FROM ANDES TO AMAZON. *Global Change Biology*, 16(12), 3176–3192. <https://doi.org/10.1111/j.1365-2486.2010.02235.x>

570 Harris, I., Jones, P., Osborn, T., & Lister, D. (2014). Updated high-resolution grids of monthly climatic
571 observations - the CRU TS3.10 Dataset: Updated high-resolution grids of monthly climatic observations.
572 *International Journal of Climatology*, *34*(3), 623–642. <https://doi.org/10.1002/joc.3711>

573 Helcoski, R., Tepley, A. J., Pederson, N., McGarvey, J. C., Meakem, V., Herrmann, V., Thompson, J. R., &
574 Anderson-Teixeira, K. J. (2019). Growing season moisture drives interannual variation in woody productivity
575 of a temperate deciduous forest. *New Phytologist*, *223*(3), 1204–1216. <https://doi.org/10.1111/nph.15906>

576 Helliker, B. R., & Richter, S. L. (2008). Subtropical to boreal convergence of tree-leaf temperatures. *Nature*,
577 *454*(7203), 511–514. <https://doi.org/10.1038/nature07031>

578 Hijmans, R. J., Cameron, S. E., Parra, J. L., Jones, P. G., & Jarvis, A. (2005). Very high resolution
579 interpolated climate surfaces for global land areas. *International Journal of Climatology*, *25*(15), 1965–1978.
580 <https://doi.org/10.1002/joc.1276>

581 Huang, M. (2019). *Air temperature optima of vegetation productivity across global biomes*. *3*, 10.

582 Hubau, W., Lewis, S. L., Phillips, O. L., Affum-Baffoe, K., Beeckman, H., Cuní-Sanchez, A., Daniels, A. K.,
583 Ewango, C. E. N., Fauset, S., Mukinzi, J. M., Sheil, D., Sonké, B., Sullivan, M. J. P., Sunderland, T. C. H.,
584 Taedoumg, H., Thomas, S. C., White, L. J. T., Abernethy, K. A., Adu-Bredu, S., ... Zemagho, L. (2020).
585 Asynchronous carbon sink saturation in African and Amazonian tropical forests. *Nature*, *579*(7797), 80–87.
586 <https://doi.org/10.1038/s41586-020-2035-0>

587 Huston, M. A., & Wolverton, S. (2009). The global distribution of net primary production: Resolving the
588 paradox. *Ecological Monographs*, *79*(3), 343–377. <https://doi.org/10.1890/08-0588.1>

589 Jian, J., Vargas, R., Anderson-Teixeira, K., Stell, E., Herrmann, V., Horn, M., Kholod, N., Manzon, J.,
590 Marchesi, R., Paredes, D., & Bond-Lamberty, B. (2020). *A restructured and updated global soil respiration*
591 *database (SRDB-V5)* [Preprint]. Data, Algorithms, and Models. <https://doi.org/10.5194/essd-2020-136>

592 Jung, M., Reichstein, M., Margolis, H. A., Cescatti, A., Richardson, A. D., Arain, M. A., Arneth, A.,
593 Bernhofer, C., Bonal, D., Chen, J., Gianelle, D., Gobron, N., Kiely, G., Kutsch, W., Lasslop, G., Law, B. E.,
594 Lindroth, A., Merbold, L., Montagnani, L., ... Williams, C. (2011). Global patterns of land-atmosphere fluxes
595 of carbon dioxide, latent heat, and sensible heat derived from eddy covariance, satellite, and meteorological
596 observations. *Journal of Geophysical Research*, *116*, G00J07. <https://doi.org/10.1029/2010JG001566>

597 Keenan, T. F., Gray, J., Friedl, M. A., Toomey, M., Bohrer, G., Hollinger, D. Y., Munger, J. W., O’Keefe,
598 J., Schmid, H. P., Wing, I. S., Yang, B., & Richardson, A. D. (2014). Net carbon uptake has increased
599 through warming-induced changes in temperate forest phenology. *Nature Climate Change*, *4*(7), 598–604.

600 <https://doi.org/10.1038/nclimate2253>

601 Kerkhoff, A. J., Enquist, B. J., Elser, J. J., & Fagan, W. F. (2005). Plant allometry, stoichiometry and the
 602 temperature-dependence of primary productivity: Plant allometry, stoichiometry and productivity. *Global*
 603 *Ecology and Biogeography*, 14(6), 585–598. <https://doi.org/10.1111/j.1466-822X.2005.00187.x>

604 Klesse, S., Babst, F., Lienert, S., Spahni, R., Joos, F., Bouriaud, O., Carrer, M., Di Filippo, A., Poulter, B.,
 605 Trotsiuk, V., Wilson, R., & Frank, D. C. (2018). A combined tree ring and vegetation model assessment of
 606 european forest growth sensitivity to interannual climate variability. *Global Biogeochemical Cycles*, 32(8),
 607 1226–1240. <https://doi.org/https://doi.org/10.1029/2017GB005856>

608 Klesse, S., DeRose, R. J., Babst, F., Black, B. A., Anderegg, L. D. L., Axelson, J., Ettinger, A., Griesbauer, H.,
 609 Guiterman, C. H., Harley, G., Harvey, J. E., Lo, Y.-H., Lynch, A. M., O’Connor, C., Restaino, C., Sauchyn,
 610 D., Shaw, J. D., Smith, D. J., Wood, L., . . . Evans, M. E. K. (2020). Continental-scale tree-ring-based
 611 projection of douglas-fir growth: Testing the limits of space-for-time substitution. *Global Change Biology*,
 612 26(9), 5146–5163. <https://doi.org/https://doi.org/10.1111/gcb.15170>

613 Kunert, N., El-Madany, T. S., Aparecido, L. M. T., Wolf, S., & Potvin, C. (2019). Understanding the controls
 614 over forest carbon use efficiency on small spatial scales: Effects of forest disturbance and tree diversity.
 615 *Agricultural and Forest Meteorology*, 269-270, 136–144. <https://doi.org/10.1016/j.agrformet.2019.02.007>

616 Larjavaara, M., & Muller-Landau, H. C. (2012). Temperature explains global variation in biomass among
 617 humid old-growth forests: Temperature and old-growth forest biomass. *Global Ecology and Biogeography*,
 618 21(10), 998–1006. <https://doi.org/10.1111/j.1466-8238.2011.00740.x>

619 Lieth, H. (1973). Primary production: Terrestrial ecosystems. *Human Ecology*, 1(4), 303–332. <https://doi.org/10.1007/BF01536729>

621 Litton, C. M., Raich, J. W., & Ryan, M. G. (2007). Carbon allocation in forest ecosystems. *Global Change*
 622 *Biology*, 13(10), 2089–2109. <https://doi.org/10.1111/j.1365-2486.2007.01420.x>

623 Li, & Xiao. (2019). Mapping Photosynthesis Solely from Solar-Induced Chlorophyll Fluorescence: A Global,
 624 fine-Resolution Dataset of Gross Primary Production Derived from OCO-2. *Remote Sensing*, 11(21), 2563.
 625 <https://doi.org/10.3390/rs11212563>

626 Luyssaert, S., Inglisma, I., Jung, M., Richardson, A. D., Reichstein, M., Papale, D., Piao, S. L., Schulze,
 627 E. D., Wingate, L., Matteucci, G., Aragao, L., Aubinet, M., Beer, C., Bernhofer, C., Black, K. G., Bonal,
 628 D., Bonnefond, J. M., Chambers, J., Ciais, P., . . . Janssens, I. A. (2007). CO₂ balance of boreal,
 629 temperate, and tropical forests derived from a global database. *Global Change Biology*, 13(12), 2509–2537.

630 <https://doi.org/10.1111/j.1365-2486.2007.01439.x>

631 Malhi, Y. (2012). The productivity, metabolism and carbon cycle of tropical forest vegetation: Carbon cycle
 632 of tropical forests. *Journal of Ecology*, 100(1), 65–75. <https://doi.org/10.1111/j.1365-2745.2011.01916.x>

633 Malhi, Y., Doughty, C., & Galbraith, D. (2011). The allocation of ecosystem net primary productivity in
 634 tropical forests. *Philosophical Transactions of the Royal Society B: Biological Sciences*, 366(1582), 3225–3245.
 635 <https://doi.org/10.1098/rstb.2011.0062>

636 Malhi, Y., Girardin, C. A. J., Goldsmith, G. R., Doughty, C. E., Salinas, N., Metcalfe, D. B., Huaraca Huasco,
 637 W., Silva-Espejo, J. E., Aguilla-Pasquell, J. del, Farfán Amézquita, filio, Aragão, L. E. O. C., Guerrieri, R.,
 638 Ishida, F. Y., Bahar, N. H. A., Farfan-Rios, W., Phillips, O. L., Meir, P., & Silman, M. (2017). The variation
 639 of productivity and its allocation along a tropical elevation gradient: A whole carbon budget perspective.
 640 *New Phytologist*, 214(3), 1019–1032. <https://doi.org/10.1111/nph.14189>

641 Martin-Benito, D., & Pederson, N. (2015). Convergence in drought stress, but a divergence of climatic
 642 drivers across a latitudinal gradient in a temperate broadleaf forest. *Journal of Biogeography*, 42(5), 925–937.
 643 <https://doi.org/https://doi.org/10.1111/jbi.12462>

644 Mau, A., Reed, S., Wood, T., & Cavaleri, M. (2018). Temperate and Tropical Forest Canopies are Already
 645 Functioning beyond Their Thermal Thresholds for Photosynthesis. *Forests*, 9(1), 47. <https://doi.org/10.3390/f9010047>

647 McDowell, N., Allen, C. D., Anderson-Teixeira, K., Brando, P., Brien, R., Chambers, J., Christoffersen, B.,
 648 Davies, S., Doughty, C., Duque, A., Espirito-Santo, F., fisher, R., Fontes, C. G., Galbraith, D., Goodsman,
 649 D., Grossiord, C., Hartmann, H., Holm, J., Johnson, D. J., . . . Xu, X. (2018). Drivers and mechanisms of
 650 tree mortality in moist tropical forests. *New Phytologist*, 219(3), 851–869. <https://doi.org/10.1111/nph.15027>

651 Michaletz, S. T., Cheng, D., Kerkhoff, A. J., & Enquist, B. J. (2014). Convergence of terrestrial plant
 652 production across global climate gradients. *Nature*, 512(7512), 39–43. <https://doi.org/10.1038/nature13470>

653 Michaletz, S. T., Kerkhoff, A. J., & Enquist, B. J. (2018). Drivers of terrestrial plant production across broad
 654 geographical gradients. *Global Ecology and Biogeography*, 27(2), 166–174. <https://doi.org/10.1111/geb.12685>

655 Millennium Ecosystem Assessment. (2005). *Ecosystems and Human Well-being: Biodiversity Synthesis* (p.
 656 100). World Resources Institute.

657 Moser, G., Leuschner, C., Hertel, D., Graefe, S., Soethe, N., & Iost, S. (2011). Elevation effects on
 658 the carbon budget of tropical mountain forests (S Ecuador): The role of the belowground compartment:

ELEVATION EFFECTS ON FOREST CARBON CYCLING. *Global Change Biology*, 17(6), 2211–2226.

<https://doi.org/10.1111/j.1365-2486.2010.02367.x>

Muller-Landau, H. C., Cushman, K., Arroyo, E. E., Martinez Cano, I., Anderson-Teixeira, K. J., & Backiel, B. (2020). Patterns and mechanisms of spatial variation in tropical forest productivity, woody residence time, and biomass. *New Phytologist*, nph.17084. <https://doi.org/10.1111/nph.17084>

Niedziałkowska, M., Kończak, J., Czarnomska, S., & Jędrzejewska, B. (2010). Species diversity and abundance of small mammals in relation to forest productivity in northeast Poland. *Écoscience*, 17(1), 109–119. <https://doi.org/10.2980/17-1-3310>

Pastorello, G., Trotta, C., Canfora, E., Chu, H., Christianson, D., Cheah, Y.-W., Poindexter, C., Chen, J., Elbashandy, A., Humphrey, M., Isaac, P., Polidori, D., Ribeca, A., van Ingen, C., Zhang, L., Amiro, B., Ammann, C., Arain, M. A., Ardö, J., . . . Papale, D. (2020). The FLUXNET2015 dataset and the ONEFlux processing pipeline for eddy covariance data. *Scientific Data*, 7(1), 225. <https://doi.org/10.1038/s41597-020-0534-3>

Piao, S., Luyssaert, S., Ciais, P., Janssens, I. A., Chen, A., Cao, C., Fang, J., Friedlingstein, P., Luo, Y., & Wang, S. (2010). Forest annual carbon cost: A global-scale analysis of autotrophic respiration. *Ecology*, 91(3), 652–661. <https://doi.org/10.1890/08-2176.1>

Potapov, P., Yaroshenko, A., Turubanova, S., Dubinin, M., Laestadius, L., Thies, C., Aksenov, D., Egorov, A., Yesipova, Y., Glushkov, I., Karpachevskiy, M., Kostikova, A., Manisha, A., Tsybikova, E., & Zhuravleva, I. (2008). Mapping the World’s Intact Forest Landscapes by Remote Sensing. *Ecology and Society*, 13(2), art51. <https://doi.org/10.5751/ES-02670-130251>

Poulter, B., Aragão, L., Andela, N., Bellassen, V., Ciais, P., Kato, T., Lin, X., Nachin, B., Luyssaert, S., Pederson, N., Peylin, P., Piao, S., Saatchi, S., Schepaschenko, D., Schelhaas, M., & Shvidenko, A. (2018). *The global forest age dataset (GFADv1.0), link to NetCDF file*. PANGAEA. <https://doi.org/10.1594/PANGAEA.889943>

R Core Team. (2020). *R: A language and environment for statistical computing*. R Foundation for Statistical Computing. <https://www.R-project.org/>

Rogelj, J., Shindell, D., Jiang, K., Fifita, S., Forster, P., Ginzburg, V., Handa, C., Kobayashi, S., Kriegler, E., Mundaca, L., Séférian, R., Vilarinho, M. V., Calvin, K., Emmerling, J., Fuss, S., Gillett, N., He, C., Hertwich, E., Höglund-Isaksson, L., . . . Schaeffer, R. (2018). *Mitigation Pathways Compatible with 1.5°C in the Context of Sustainable Development*. 82.

689 Rutishauser, E., Wright, S. J., Condit, R., Hubbell, S. P., Davies, S. J., & Muller-Landau, H. C. (2020). Testing
690 for changes in biomass dynamics in large-scale forest datasets. *Global Change Biology*, 26(3), 1485–1498.
691 <https://doi.org/10.1111/gcb.14833>

692 Schuur, E. A. G. (2003). Productivity and global climate revisited: The sensitivity of trop-
693 ical forest growth to precipitation. *Ecology*, 84(5), 1165–1170. [https://doi.org/10.1890/0012-](https://doi.org/10.1890/0012-9658(2003)084[1165:PAGCRT]2.0.CO;2)
694 [9658\(2003\)084\[1165:PAGCRT\]2.0.CO;2](https://doi.org/10.1890/0012-9658(2003)084[1165:PAGCRT]2.0.CO;2)

695 Slot, M., & Winter, K. (2018). High tolerance of tropical sapling growth and gas exchange to moderate
696 warming. *Functional Ecology*, 32(3), 599–611. <https://doi.org/10.1111/1365-2435.13001>

697 Smith, M. N., Taylor, T. C., Haren, J. van, Rosolem, R., Restrepo-Coupe, N., Adams, J., Wu, J., Oliveira, R.
698 C. de, Silva, R. da, Araujo, A. C. de, Camargo, P. B. de, Huxman, T. E., & Saleska, S. R. (2020). Empirical
699 evidence for resilience of tropical forest photosynthesis in a warmer world. *Nature Plants*, 6(10), 1225–1230.
700 <https://doi.org/10.1038/s41477-020-00780-2>

701 Sullivan, M. J. P., Lewis, S. L., Affum-Baffoe, K., Castilho, C., Costa, F., Sanchez, A. C., Ewango, C. E. N.,
702 Hubau, W., Marimon, B., Monteagudo-Mendoza, A., Qie, L., Sonké, B., Martinez, R. V., Baker, T. R., Brien, R. J. W.,
703 Feldpausch, T. R., Galbraith, D., Gloor, M., Malhi, Y., . . . Phillips, O. L. (2020). Long-term thermal
704 sensitivity of Earth’s tropical forests. *Science*, 368(6493), 869. <https://doi.org/10.1126/science.aaw7578>

705 Šímová, I., & Storch, D. (2017). The enigma of terrestrial primary productivity: Measurements, models, scales
706 and the diversity-productivity relationship. *Ecography*, 40(2), 239–252. <https://doi.org/10.1111/ecog.02482>

707 Taylor, P. G., Cleveland, C. C., Wieder, W. R., Sullivan, B. W., Doughty, C. E., Dobrowski, S. Z., &
708 Townsend, A. R. (2017). Temperature and rainfall interact to control carbon cycling in tropical forests.
709 *Ecology Letters*, 20(6), 779–788. <https://doi.org/10.1111/ele.12765>

710 Trabucco, A., & Zomer, R. J. (2019). *Global Aridity Index and Potential Evapo-Transpiration (ET0) Climate*
711 *Database v2*. 10. <https://doi.org/10.6084/m9.figshare.7504448.v3>

712 Vlam, M., Baker, P. J., Bunyavejchewin, S., & Zuidema, P. A. (2014). Temperature and rainfall strongly
713 drive temporal growth variation in Asian tropical forest trees. *Oecologia*, 174(4), 1449–1461. [https://doi.org/](https://doi.org/10.1007/s00442-013-2846-x)
714 [10.1007/s00442-013-2846-x](https://doi.org/10.1007/s00442-013-2846-x)

715 Wagner, F. H., Hérault, B., Bonal, D., Stahl, C., Anderson, L. O., Baker, T. R., Becker, G. S., Beeckman, H.,
716 Boanerges Souza, D., Botosso, P. C., Bowman, D. M. J. S., Bräuning, A., Brede, B., Brown, F. I., Camarero,
717 J. J., Camargo, P. B., Cardoso, F. C. G., Carvalho, F. A., Castro, W., . . . Aragão, L. E. O. C. (2016).
718 Climate seasonality limits leaf carbon assimilation and wood productivity in tropical forests. *Biogeosciences*,

13(8), 2537–2562. <https://doi.org/10.5194/bg-13-2537-2016>

Wagner, F., Rossi, V., Aubry-Kientz, M., Bonal, D., Dalitz, H., Gliniars, R., Stahl, C., Trabucco, A., & Hérault, B. (2014). Pan-Tropical Analysis of Climate Effects on Seasonal Tree Growth. *PLoS ONE*, 9(3), e92337. <https://doi.org/10.1371/journal.pone.0092337>

Waide, R. B., Willig, M. R., Steiner, C. F., Mittelbach, G., Gough, L., Dodson, S. I., Juday, G. P., & Parmenter, R. (1999). The Relationship Between Productivity and Species Richness. *Annual Review of Ecology and Systematics*, 30(1), 257–300. <https://doi.org/10.1146/annurev.ecolsys.30.1.257>

Wei, W., Weile, C., & Shaopeng, W. (2010). Forest soil respiration and its heterotrophic and autotrophic components: Global patterns and responses to temperature and precipitation. *Soil Biology and Biochemistry*, 42(8), 1236–1244. <https://doi.org/10.1016/j.soilbio.2010.04.013>

Xia, J., Yuan, W., Lienert, S., Joos, F., Ciais, P., Viovy, N., Wang, Y.-p., Wang, X., Zhang, H., Chen, Y., & Tian, X. (2019). Global patterns in net primary production allocation regulated by environmental conditions and forest stand age: A model-data comparison. *Journal of Geophysical Research: Biogeosciences*, 124(7), 2039–2059. <https://doi.org/https://doi.org/10.1029/2018JG004777>

Yu, G., Chen, Z., Piao, S., Peng, C., Ciais, P., Wang, Q., Li, X., & Zhu, X. (2014). High carbon dioxide uptake by subtropical forest ecosystems in the East Asian monsoon region. *Proceedings of the National Academy of Sciences*, 111(13), 4910–4915. <https://doi.org/10.1073/pnas.1317065111>

Zak, D. R., Tilman, D., Parmenter, R. R., Rice, C. W., fisher, F. M., Vose, J., Milchunas, D., & Martin, C. W. (1994). Plant Production and Soil Microorganisms in Late-Successional Ecosystems: A Continental-Scale Study. *Ecology*, 75(8), 2333. <https://doi.org/10.2307/1940888>

Zani, D., Crowther, T. W., Mo, L., Renner, S. S., & Zohner, C. M. (2020). *Increased growing-season productivity drives earlier autumn leaf senescence in temperate trees*. 7.

Zhao, M., Heinsch, F. A., Nemani, R. R., & Running, S. W. (2005). Improvements of the modis terrestrial gross and net primary production global data set. *Remote Sensing of Environment*, 95(2), 164–176. <https://doi.org/https://doi.org/10.1016/j.rse.2004.12.011>

Zhou, S., Zhang, Y., Caylor, K. K., Luo, Y., Xiao, X., Ciais, P., Huang, Y., & Wang, G. (2016). Explaining inter-annual variability of gross primary productivity from plant phenology and physiology. *Agricultural and Forest Meteorology*, 226–227, 246–256. <https://doi.org/10.1016/j.agrformet.2016.06.010>